The Effect of Sheet Processing on the Elevated Temperature Strength and Creep Behavior of INCONEL® Alloy 718

BY

DANIEL S. DICKMANN

A THESIS
SUBMITTED TO THE FACULTY OF

ALFRED UNIVERSITY

IN PARTIAL FULFILLMENT OF THE REQUIREMENTS
FOR THE DEGREE OF

MASTER OF SCIENCE

IN

MATERIALS SCIENCE AND ENGINEERING

ALFRED, NEW YORK

April, 2004

The Effect of Sheet Processing on the Elevated Temperature Strength and Creep Behavior of INCONEL® Alloy 718

BY

DANIEL S. DICKMANN

B.S. ALFRED UNIVERSITY (2003)

SIGNATURE OF AUTHOR (Signature on file)

APPROVED BY (Signature on file)
CARL BOEHLERT, ADVISOR

(Signature on file)
ALAN MEIER, ADVISORY COMMITTEE

(Signature on file)
CASPAR McCONVILLE, ADVISORY COMMITTEE

(Signature on file)
DOREEN EDWARDS, CHAIR, ORAL THESIS DEFENSE

ACCEPTED BY (Signature on file)
ALASTAIR CORMACK, DEAN,
SCHOOL OF ENGINEERING

ACKNOWLEDGMENTS

I would like to thank Dr. Carl Boehlert for his help and support. Special thanks to Special Metals Corporation and Nate Eisienger who provided the material to make this project possible. I would like to acknowledge all the undergraduates whose help was invaluable with this project including Istvan Szabo, Daniel Burnett, and Mike Hanes. Finally, I would like to thank my wife whose unwavering faith and support make everything I do possible.

TABLE OF CONTENTS

LIST OF TABLES

LIST OF FIGURES

ABSTRACT

The grain size, creep, and elevated temperature tensile behavior of INCONEL® alloy 718 (IN 718) were investigated to identify processing-microstructure-property relationships. The alloy was cold rolled (CR) 0-80% followed by annealing at 954°C or 1050°C and then by aging using the traditional aging schedule for this alloy. This alloy can be superplastically formed (IN 718SPF) to a significantly finer grain size and this condition was also evaluated. The creep behavior was evaluated in the applied stress range 300-758 MPa at a temperature of 638°C. Constant-load tensile creep experiments were used to measure the values of the steady-state creep rate and the consecutive load reduction method was used to determine the values of backstress, σ_o. Tensile tests were also performed at 650°C.

For the 954°C annealed samples, The 20%CR and 30%CR samples exhibited the greatest σ_0 values, 645 and 630 MPa, respectively, while the 60%CR and 80%CR conditions exhibited the lowest σ_0 values, which were less than half those of the highest σ_0 values. The creep resistance after 60-80%CR was significantly worse than conventionally processed and 10%CR conditions, which is expected based on the finer grain size of the heavily CR samples. For the 1050°C annealed samples, the SPF sample exhibited the greatest σ_0 value, 630 MPa, while the 0%CR condition exhibited the lowest σ_0 value, 450 MPa. The backstress values for most of the 1050°C annealed samples fell in a narrow band, 550-590 MPa. For most samples, the backstress was over 50% of the yield stress at 650°C. Overall, the 20%CR and 30%CR conditions exhibited the best elevated temperature properties in the 954°C annealed condition while the IN 718SPF exhibited exceptional strength and creep resistance in the 1050°C annealed condition, on par with the 20-30%CR 954°C annealed samples.

A transition in the effective stress exponent occurred independent of annealing temperature at an effective stress of approximately 135 MPa. The data suggested that the creep mechanism was dependent on the effective stress and indicated that diffusional creep or grain boundary sliding may be active at effective stresses lower than 135MPa.

® INCONEL is a registered trademark of Special Metals Corporation.

I INTRODUCTION

INCONEL® alloy 718 (IN 718) is a precipitation hardenable nickel-chromium alloy containing significant amounts of iron, niobium, and molybdenum along with other elements.[1,2] IN718 has an austenitic equiaxed face-centered cubic matrix, γ. The major strengthening phases are γ' and γ" which are dispersed throughout the γ phase. A fine coherent spherical face-centered cubic precipitate, γ' consists of Ni_3Al with Ti and Nb as possible substitutes for the Al.[1,2] Most of the strengthening can be contributed to γ", a coherent ordered disc-shaped body-centered tetragonal precipitate consisting of Ni_3Nb with Al and Ti as possible substitutes for the Nb.[1,2] An orthorhombic phase, δ, consisting of Ni_3NB can also be found at grain boundaries.[1]

The ease and economy with which IN 718 can be fabricated, combined with good tensile, fatigue, creep and rupture strength at temperatures up to 700°C, have resulted in its use in a wide range of applications including components for liquid rockets, aircraft turbine engines, cryogenic tanks, spacecraft, nuclear reactors, pumps and tooling.[1,2] Some examples of these properties are room temperature tensile and yield strength exceeding 1400 MPa and 1300 MPa respectively with elongations up to 25% and a creep rupture life exceeding 1000 hrs at 650°C and stresses exceeding 800 MPa.[1]

Although the properties of IN 718 are excellent, there is room for improvement. The purpose of this study was to determine the processing-microstructure-property relationships of IN 718. Although this alloy is over 50 years old, few published works have concentrated on the creep behavior and especially the creep backstress of IN 718. This work is focused on the creep behavior and in particular the creep backstress of IN 718 and the following description will include background on both these topics.

A. Basic Creep Theory

For pure metals, it has been shown that at a constant temperature (greater than 0.4 the melting temperature) the steady-state creep rate varies with applied stress, σ_a, as follows (where B is a constant and n is the creep stress exponent):[3]

$$\varepsilon_{ss} = B\sigma_a^{\,n} \qquad (1)$$

Therefore, by plotting the steady-state creep rate versus the applied stress on a log-log scale a straight line results. At low stresses, an n value of approximately 1 is achieved (Figure 1).[3] In this regime, the creep process is controlled by stress directed atomic diffusion.[4] At intermediate to high stress levels, creep is believed to be controlled by diffusion controlled movement of dislocations. In this regime, an n value of approximately 5 is reached (Figure 1).[4]

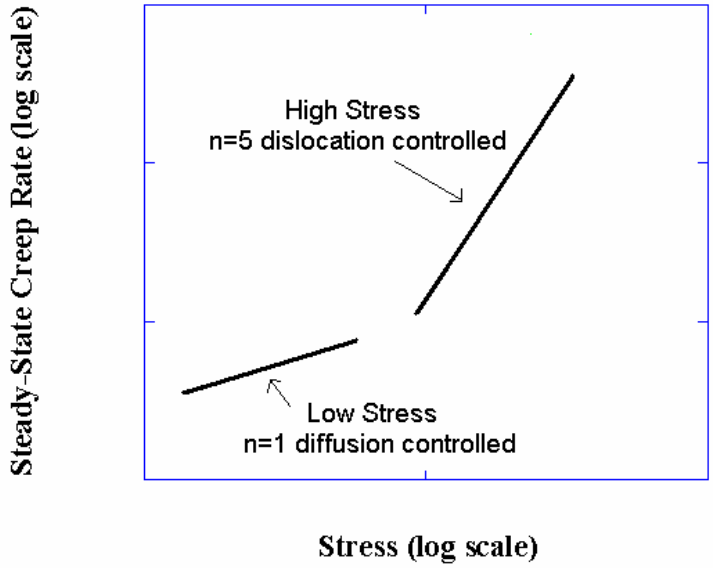

Figure 1. Schematic illustrating the creep stress exponent, n, values for the diffusion and dislocation controlled creep regimes for pure metals.

B. Advanced Creep Theory Including Backstress

The creep mechanisms that operate during elevated-temperature deformation of pure metals and solid-solution strengthened alloys have been related to the value of the stress exponent, n_a, and the apparent activation energy, Q_a, in the Dorn steady-state creep rate equation:[5]

$$\varepsilon_{ss} = A\, D_o \exp(-Q_a/RT)\, \mu b/kT\, (\sigma_a/\mu)^{n_a} \qquad (2)$$

where T is the creep temperature in degrees K, R is the gas constant, and A is often referred to as the Dorn constant, b is Burger's vector, D_o is the pre-exponential factor, μ is the shear modulus, and k is the Boltzmann constant. However, the n_a and Q_a values measured for most commercial alloys containing dispersed second-phase particles are considerably greater than those observed in pure metals and solid solution strengthened alloys.[6-17] The n_a values for precipitation-hardened alloys have ranged between 5-15[6-10] while, for dispersion-hardened alloys, including thoria dispersed Ni-20Cr (wt.%), n_a values have ranged between 9-75.[13,16,17] The Q_a values have ranged from one to three times those of the activation energy for self diffusion.[15,17,18] These variations in the observed values of n_a and Q_a have been rationalized by introducing the concept of a backstress or threshold stress, σ_o, which is an internal stress opposing the dislocation motion. In multiphase phase alloys such as IN 718, which contains an austenitic FCC phase matrix (γ) and fine γ' and γ" strengthening precipitates, the applied stress during steady-state creep deformation is opposed by a backstress resulting from the presence of these strengthening particles and a defect structure within the material.[6,13,19-24] Therefore, the creep deformation results from an effective stress ($\sigma_e=\sigma_a-\sigma_o$). As a result, the steady-state creep rate can be represented by:

$$\varepsilon_{ss} = A^*(\sigma_a - \sigma_o)^{n_e} \qquad (3)$$

where n_e is the effective stress exponent. Although traditionally used to measure the backstress during dislocation power law creep, it has been shown that the consecutive

stress reduction method can also be applied to diffusional creep for IN 718 where low n_e values are observed.[19,20]

The mechanism of diffusional creep in particle-strengthened alloys is different from that of single-phase alloys or pure metals. Diffusional creep in the latter is known to be the result of stress-induced diffusion or the migration of matter from grain boundaries that are in tension to those that are in compression. In contrast, in particle-strengthened alloys, diffusion of vacancies will be inhibited by the precipitate particles with an accumulation of vacancies at the precipitate-matrix interface and a resultant build-up of stress concentration. This stress concentration at the interface can be relaxed by the punching of prismatic dislocation loops in the matrix, which can annihilate themselves by the absorption of vacancies.[25,26]

Therefore to accommodate even very limited diffusional strain, in particle-strengthened alloys, additional plastic deformation must occur around precipitates either in the grain boundary region or within grains, giving an n_e value slightly greater than 1. Furthermore, according to Ansel and Weertman,[27] diffusional creep can involve the process of dislocation climb over the particles. Therefore, diffusional creep in particle-strengthened alloys can involve not only vacancy diffusion in the matrix and dislocation motion in the grain boundary region but also dislocation creation and motion within the grains. Ansel and Weertman[27] considered the rate controlling process to be the climb of dislocations over the precipitate particles, which also depends on the diffusion rate.

However, if cross-slip is also important in the above process, the creep rate will be more sensitive to stress. Han and Chaturvedi[20] observed dislocation segments and loops within grains even under the testing conditions where they considered diffusional creep to occur. Their observations suggest that the creep rate is more sensitive to the applied stress in particle-strengthened alloys than to that in pure metals; i.e. the value of n_e can be slightly greater than 1. This observation is in agreement with the findings of Ansel and Weertman.[27]

The existence of a transition region between diffusional creep and homogeneous power-law creep has been suggested by Ashby and Frost.[28] They considered diffusional flow as grain boundary sliding with diffusional accommodation. During this process, incompatibility generated by grain boundary sliding is removed at a steady-state rate by

diffusion of atoms from sources on some grain boundaries to sinks on other grain boundaries. If the strain rate is increased sufficiently, diffusion can no longer accommodate the sliding and a nonuniform power-law creep within grains, called "folds", appears. As the strain rate increases further, flow becomes increasingly uniform and the folds disappear. This process leads to homogeneous power law creep. The region where diffusion can no longer accommodate the grain boundary sliding and nonuniform power law creep appears is designated as a transition region between diffusional and power law creep.

The higher the backstress, the more creep resistant the material. By finding the ideal processing conditions, the creep properties of IN 718 can be maximized. Since IN 718 is often used in aerospace applications, even a small improvement in properties can be very significant. Any reduction in weight is important for aerospace applications. Also, improved properties can lead to higher use temperatures for jet engines. This improves efficiency and leads to further savings. For example, a single W501G power generating gas turbine would be expected to exhibit a 0.7% increase in efficiency when the operating temperature is increased 50°C. This increase in efficiency could result in a savings of $300,000 a year from reduced fuel consumption and another $65,000 a year due to reduced emissions.[29] Although the backstress of IN 718 has been studied in the as processed condition,[19,20] to the author's knowledge the effect of thermomechanical processing on the backstress of IN 718 had not been systematically examined before this study.

II EXPERIMENTAL PROCEDURE

In order to determine the effects of cold rolling and annealing temperature on the elevated temperature mechanical properties of IN 718, a series of tensile creep and elevated temperature tensile experiments were performed on thermomechanically processed (TMP) sheets. The IN 718 sheets used in this study were processed at Special Metals Corporation, Huntington, WV using its commercial grade composition. The heats were produced by vacuum induction melting followed by electroslag remelting. The material was hot worked using conventional practices and the as-processed condition included mill annealing at 1066°C for all hot-rolling procedures which preceded the final cold rolling (CR) and annealing.

Subsequent TMP treatments included CR between 10-80%. The CR steps were performed on separate sheets each designated with 10%, 20%, 30%, 40,%, 60%, and 80% deformation. The annealing treatments were performed at 954 or 1050°C. The aging treatment consisted of 718˚C/8h/furnace cool to 621˚C then hold at 621˚C for a total aging time of 18h. This aging treatment is intended to precipitate out the γ' and γ" strengthening phases. In addition, a separate sheet of IN 718SPF was produced in a similar fashion, however the sheet cold working procedure, estimated to total between 55-80% deformation, was altered to assure the production of an ultra fine grain size product.[30-33] The cold rolling levels were chosen to encompass the range of cold rolling used in industry from the convention (0%CR) to the upper limit of SPF samples (80%CR). The conventional annealing temperature for IN718 is 954°C.[1] Therefore, this temperature was chosen as one of annealing temperature variables. The other annealing temperature (1050°C) was chosen to insure grain growth so grain size could be examined to determine its affect if any on IN718's mechanical behavior.

Flat dogbone-shaped tensile and creep specimens with a cross-section of approximately 1 mm x 12 mm and a gage length of 25 mm were machined, using either a mill or an electrodischarge machine, with the tensile axis parallel to the rolling direction. The tensile experiments were performed in air at 650°C using an Instron 8562 machine and a strain rate of approximately 1.3 $x10^{-4}$ s^{-1}. Specimens were soaked at temperature

for at least 15 minutes to equilibrate temperature prior to testing. Multiple tests were performed and average yield strength, ultimate tensile strength and strain to failure were recorded.

Constant-load creep experiments were performed on an Applied Test Systems (ATS), Incorporated lever-arm creep apparatus, using a 20:1 load ratio, in air at a temperature of 638°C and applied stresses ranging between 300-758 MPa. The creep strain was monitored during the tests using a linear variable differential transformer (LVDT) attached to the gage section. The specimen temperature, monitored by three thermocouples located within the gage section during the creep experiments, was maintained within $\pm$3°C using a three-zone ATS furnace. A photo of the creep testing apparatus used in this study is presented in Figure 2.

Figure 2. The creep testing apparatus used in this study.

The σ_0 values were determined at 638°C by the consecutive stress reduction method (Figure 3).[6,8,12] When the creep rate for a given σ_a remained constant for at least five hours, it was assumed the steady-state creep rate had been achieved. Thereafter, the sample was subjected to a small stress reduction (approximately 5% σ_a). This resulted in an elastic contraction of the sample, followed by an incubation period with a zero creep rate. After a period of time, creep began again at a lower rate. Once steady state was reached, another stress reduction was performed. The time of the incubation period following each stress reduction was recorded. The remaining stress vs. the cumulative incubation time was plotted on a linear scale, and σ_o was determined by taking the asymptotic value of the remaining stress when the cumulative incubation time appeared to be infinite. It is important to note that strain rate versus stress behavior was also recorded in addition to σ_o using this method.

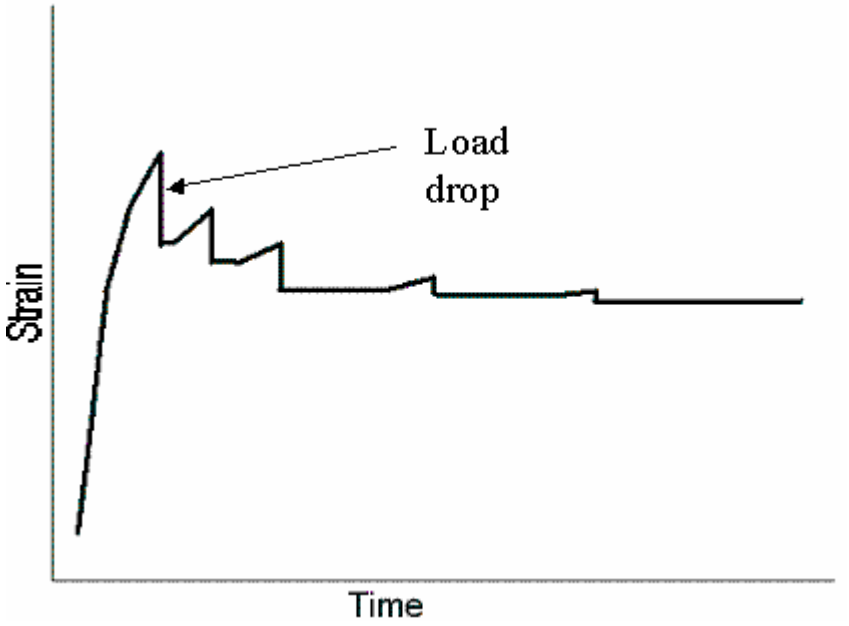

Figure 3. Strain vs. Time curve demonstrating the consecutive stress reduction method for determining backstress.

The σ_o and ε_{ss} values proved to be repeatable as duplicate samples were tested at the same temperature and σ_a and the measured ε_{ss} values were within five percent of each other. In addition, the σ_o and ε_{ss} values were not dependent on strain history for total creep strains less than 0.5% as several temperature and σ_a conditions were performed,

some in duplicate, before that of the backstress condition and in each case similar σ_o values were recorded. A summary of the mechanical tests performed is presented in Table I.

Table I. Summary of Mechanical Tests Performed

	Creep at 638°C		Tensile at 650°C	
	Annealing Temperature			
CR	954°C	1050°C	954°C	1050°C
0%	1	4	1	2
10%	2	2	3	1
20%	3	3	1	1
30%	1	1	2	1
40%	3	2	1	1
60%	1	2	1	1
80%	1	1	1	2
SPF	3	1	1	2

Scanning electron microscopy (SEM) and optical microscopy samples that were evaluated after processing and deformation were prepared by mechanical polishing and then etching using an acid solution consisting of 46 ml HCl, 2.5 ml HNO_3, and 1.5ml H_2SO_4. Etching times averaged approximately one minute. Grain size was calculated using the line intercept method on optical micrographs and confirmed on SEM micrographs.[34] SEM micrographs were also examined for evidence of cracking. Transmission electron microscopy (TEM) samples were prepared using a Struers TenuPol-5 electropolisher and a 5% perchloric acid / 95% ethyl alcohol solution. A polishing temperature of approximately -25˚C was used. Prior to electopolishing, the samples were ground to a thickness of approximately 200 μm using consecutively finer grits of SiC paper and then discs 3 mm in diameter were punched. The TEM samples were examined using a JEOL-FX TEM and an operating voltage of 120 kV to confirm the presence of fine precipitates and to complete preliminary work for future studies.

III RESULTS AND DISCUSION

A. Microstructure

The chemical composition range of the IN 718 sheets used is shown in Table II.

Table II. Composition Range in Weight Percent for the IN 718 Used in This Study[1]

Nickel 53.68-53.48	Titanium 1.01-1.06	Molybdenum 2.99	Cobalt 0.03-0.12
Chromium 18.1-18.4	Aluminum 0.46-0.48	Phosphorus 0.009-0.012	Carbon 0.03
Iron 17.99-18.3	Copper 0.02-0.17	Silicon 0.01-0.17	Manganese 0.04-0.12
Niobium (plus Tantalum) 5.07- 5.11	Sulfur 0.001		

The annealed microstructures contained an equiaxed γ-phase (FCC) austenitic matrix and after aging fine γ' (coherent spherical fcc (L_{12})) and γ" (coherent ordered disc-shaped body-centered tetragonal (DO_{22})) precipitated throughout[20] which is demonstrated in Figure 4. The γ" phase is the major strengthening phase and has an average volume fraction of about 13%.[20] Phases were visually identified only.

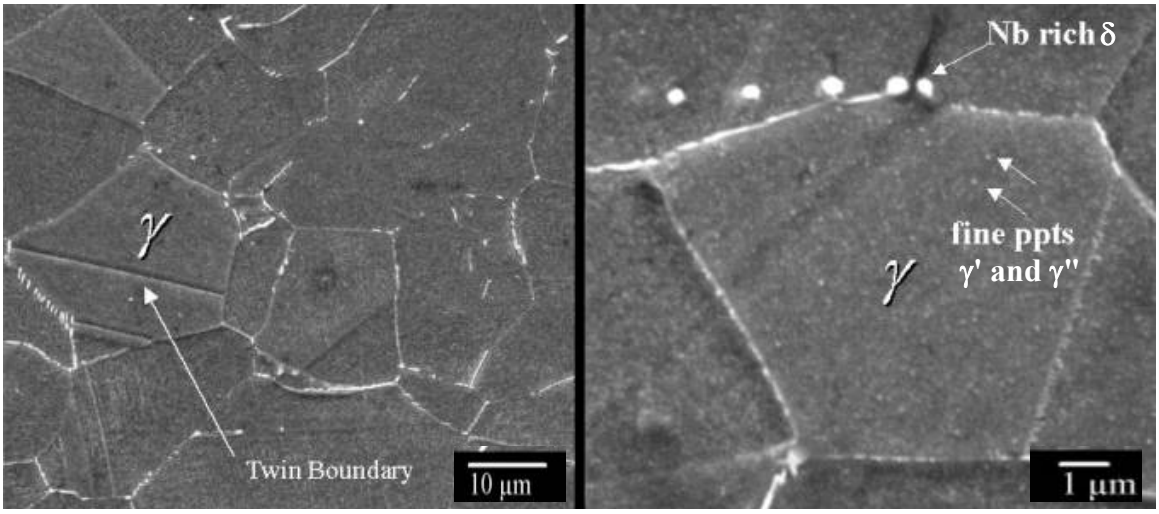

Figure 4. Low-magnification (left) and high-magnification (right) SEM photomicrographs of the cross-section of a 0% cold rolled then 954°C annealed and aged microstructure illustrating the austenitic γ-phase matrix, fine γ' and γ'' precipitates, and δ-phase precipitates.

1. Grain Size

Both annealing temperature and cold rolling deformation had a significant effect on grain size, GS (Table III). Above 1010°C, grain growth occurs[1] and the 1050°C, one-hour annealed samples exhibited an average growth in grain diameter of 61 μm (Figure 5).

Table III. Grain Size of IN 718 as a Function of Cold Rolling and Annealing

	954°C Annealed			1050°C Annealed		
CR	GS (um)	std. dev. (um)	# of grains	GS (um)	std. dev. (um)	# of grains
0%	36.2	6.6	626	92.0	11.0	31
10%	37.5	8.2	609	77.5	14.0	46
20%	30.6	6.5	748	89.1	15.3	48
30%	28.9	3.4	775	76.4	10.1	56
40%	28.7	2.5	776	83.9	8.9	34
60%	23.0	4.0	20	101.8	13.3	42
80%	20.0	3.2	23	99.8	13.3	50
SPF	12.0	1.4	238	83.9	5.7	34

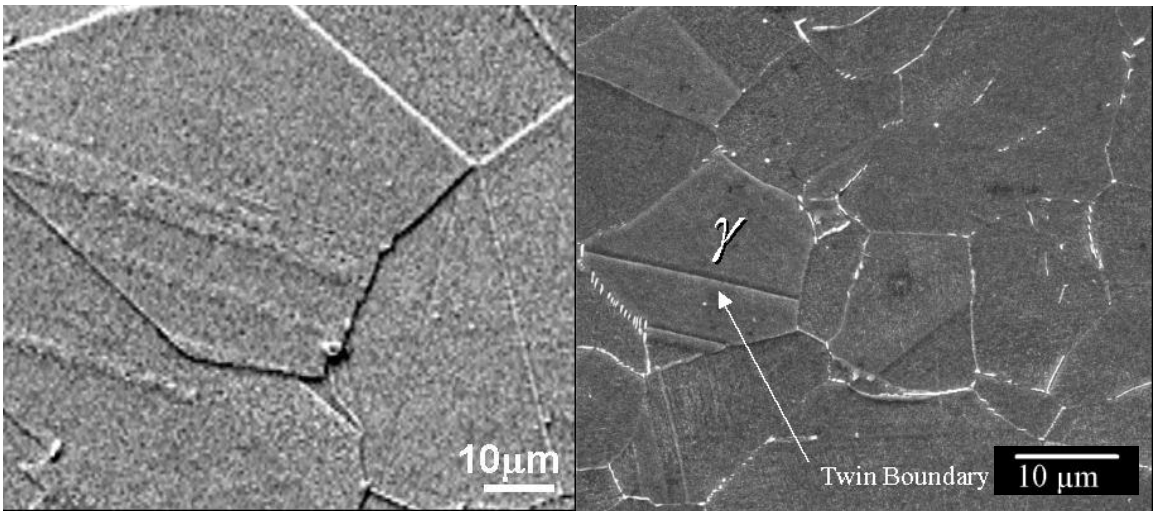

Figure 5. SEM photomicrographs of the cross-section of a 0% cold rolled then either 954°C (right) or 1050°C (left) annealed and aged sample illustrating the on average 61 μm grain growth with increased annealing temperature.

Cold rolling also had a significant effect on the grain size (Figure 6). In Figure 6 and future figures, SPF samples (55-80%CR) are represented as 70%CR. For the 954°C annealed samples, there is a general decrease in the grain size with increased cold rolling. For the 1050°C annealed samples, there is less overall change in the grain size with increased cold rolling. Between 0-40%CR, there is a slight decrease in grain size, while further cold rolling appears to increase the average grain size. Considering the uncertainty in the grain size measurement, an almost uniform or constant grain size could be depicted for the 1050°C annealed samples.

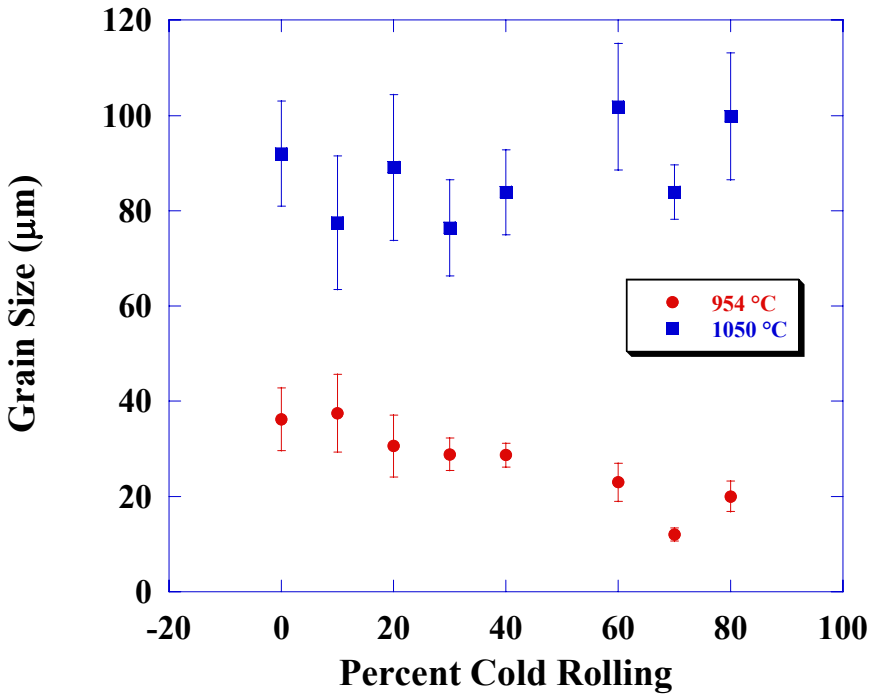

*SPF samples (55-80%CR) are represented in figure at 70%CR.

Figure 6. The effect of cold rolling on the grain size of IN 718 for samples annealed at 954°C or 1050°C. The error bars represent the uncertainty in the grain size measurement (one standard deviation of the mean).

2. TEM

The fine precipitates mentioned previously (γ' and γ") are shown in Figure 7. The TEM photo is presented to more clearly illustrate the presence of fine precipitates with the γ phase.

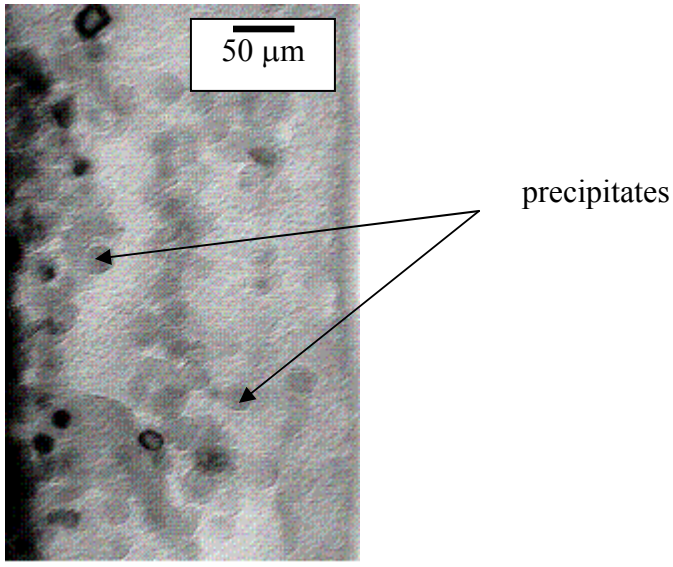

Figure 7. TEM image of an 80%CR 1050°C sample showing fine γ' and γ" precipitates.

B. Tensile Experiments

Elevated temperature tensile tests were performed to determine the effect of TMP on the yield strength (YS) and ultimate tensile strength (UTS) of IN 718. Strain-to-failure (ε_f) was also recorded (Table IV). As shown in Figure 8, for the 954°C annealed samples the strengths (UTS and YS) increased with cold rolling up to 40%CR followed by a slight decrease in strength with further cold rolling. For the 1050°C annealed samples, the YS decreased slightly with increased cold rolling and the UTS increased slightly with cold rolling.

Table IV. The 650°C Tensile Data of IN 718 TMP Samples

Cold Rolling Deformation,%	**$\sigma_{0.2\%YS}$, MPa**	**σ_{uts}, MPa**	**ε_f, %**
954°C anneal*			
0	988	1145	13.5
10	957	1115	10.8
20	1002	1184	11.4
30	959	1161	12.6
40	1054	1153	12.7
60	940	1004	2.7^
80	948	1057	19.6
SPF	991	1056	4.8^
1050°C anneal*			
0	899	1028	10.1
10	921	1041	8.1
20	878	1044	7.4
30	906	1054	14.0
40	888	1024	11.8
60	865	1036	12.7
80	876	1054	15
SPF	913	1088	12

* All samples were aged according to the aging treatment 718˚C for 8 hours followed by furnace cooling to 621°C and holding for total aging time of 18 hr; ^ sample(s) broke outside of gage section.

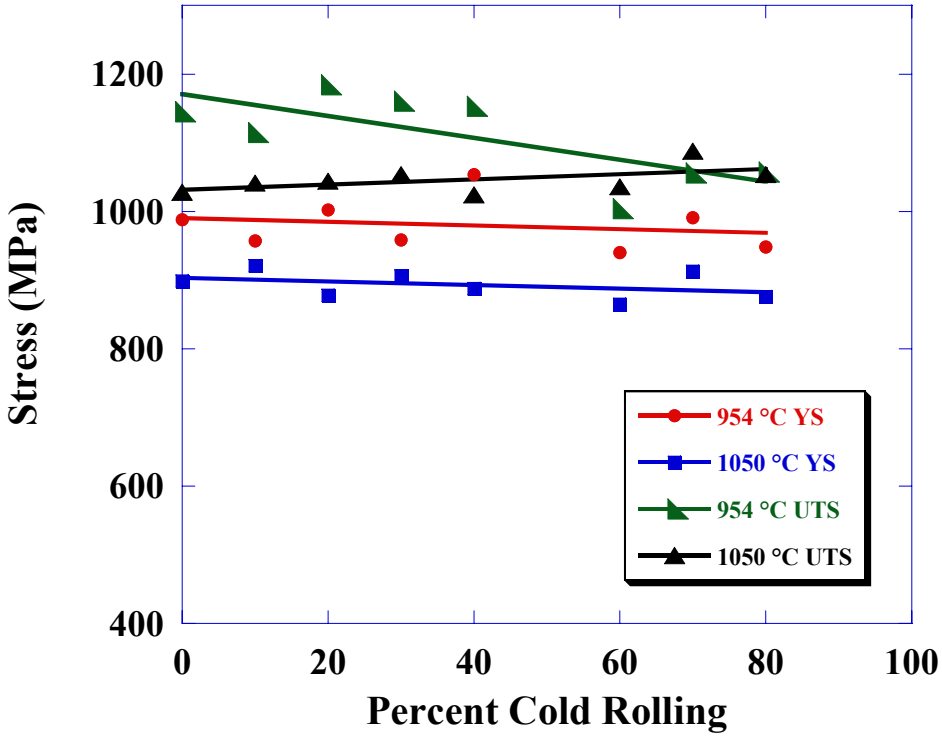

*SPF samples (55-80%CR) are represented in figure at 70%CR.

Figure 8. YS and UTS as a function of cold rolling for the 954°C and 1050°C annealed then aged samples.

C. Creep Experiments

A series of elevated temperature creep experiments were performed in order to determine the effects of TMP on the creep and backstress behavior of IN 718. Both load versus time and strain versus time were monitored (Figures 9 and 10) during all tests. Note that in Figures 9 and 10 the strain rate value at 617 MPa is nearly the same regardless if it was found during a load jump test or a load drop test (7.1E-9 s^{-1} vs. 7.2E-9 s^{-1}). The strain rate values for all the creep tests and conditions performed are presented in the appendix.

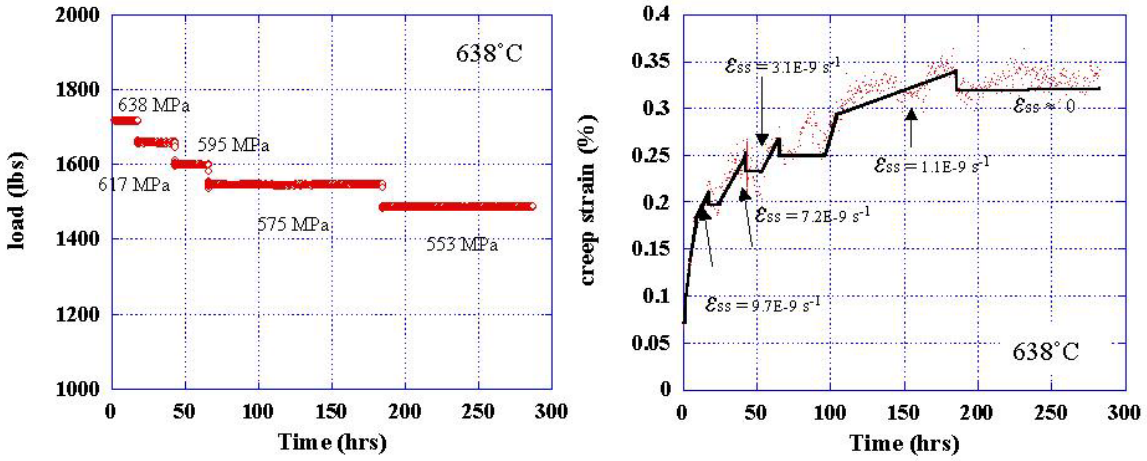

Figure 9. Load vs time and strain vs time profiles of a typical consecutive stress reduction test used to determine backstress (sample was 40%CR and annealed at 1050°C).

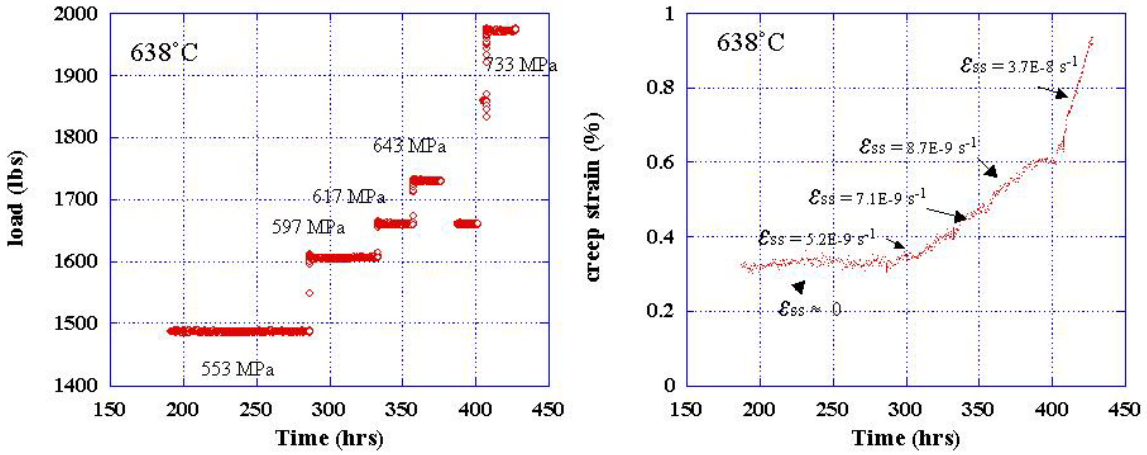

Figure 10. Typical load vs. time and strain vs. time profiles of a load jump creep test used to determine the creep stress exponent (sample was 40%CR and annealed at 1050°C).

1. 954 ˚C Annealed Samples

Backstress and n values for all cold rolling levels were determined for the 954°C annealed then aged samples (Figures 11-14). As shown in Figure 11, The 20%CR and 30%CR samples exhibited the greatest σ_0 values, 645 and 630 MPa, respectively, while the 60%CR and 80%CR conditions exhibited the lowest σ_0 values, which were less than

half those of the highest σ_0 values. The 20%CR and 30%CR conditions also exhibited the lowest strain rates for a given applied stress level.

The samples cold rolled between 10-40% exhibited greater σ_0 values than the 0%CR baseline condition, however cold rolling beyond 40% proved detrimental to the elevated-temperature strength and creep resistance, and lower σ_0 values were exhibited for such samples compared with the baseline. The significant drop in the backstress for the samples CR to greater than 40% may have been partially related to the decreased grain size (Table III). The n_a values ranged from 4 to 40 and the n_e values ranged from 1 to 4 (Figures 12-14).

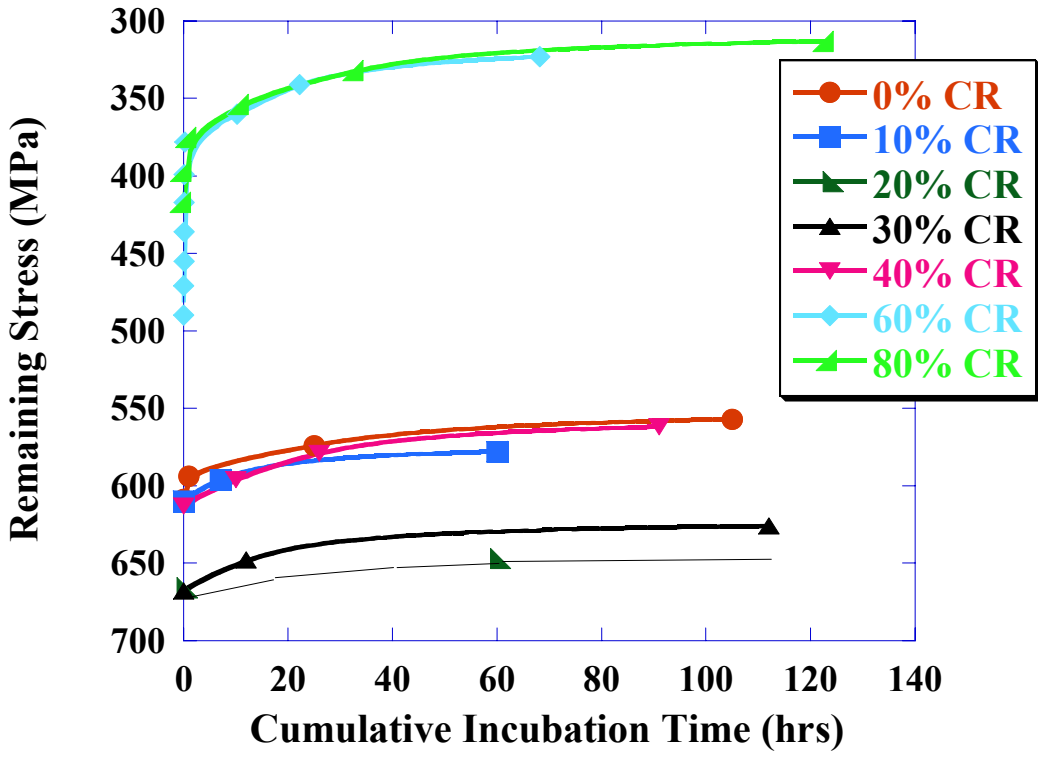

Figure 11. Remaining stress versus cumulative incubation time for the cold rolled and 954°C annealed then aged IN 718 creep samples.

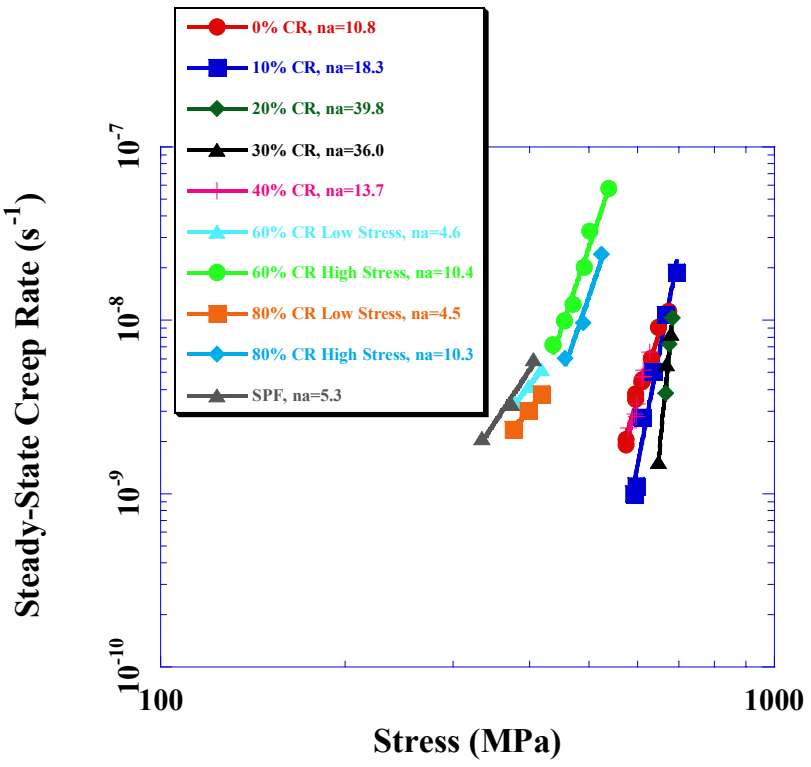

Figure 12. Steady-state creep rate versus applied stress for the cold rolled and 954°C annealed then aged IN 718 samples.

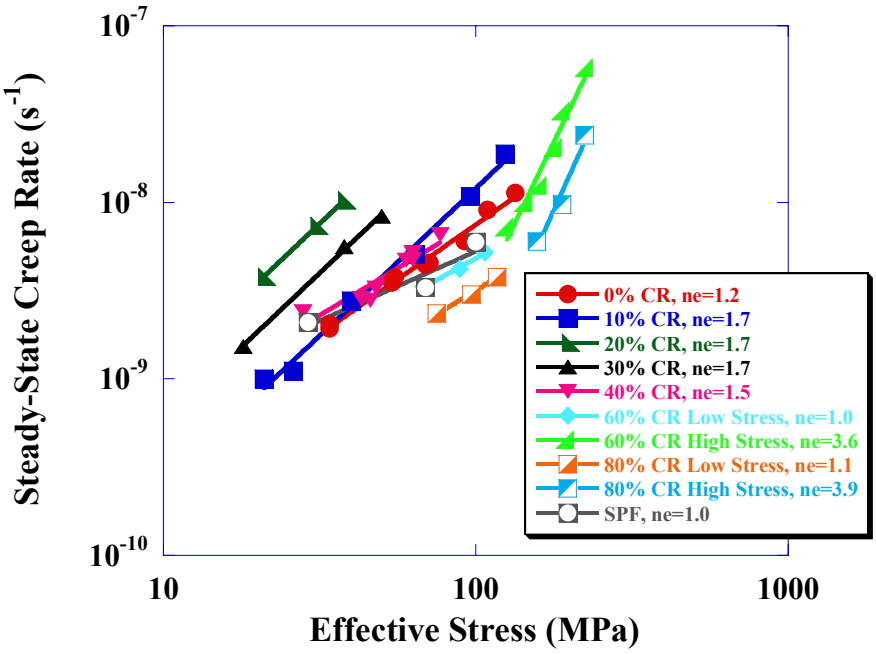

Figure 13. Steady-state creep rate versus effective stress for the cold rolled and 954°C annealed then aged IN 718 samples.

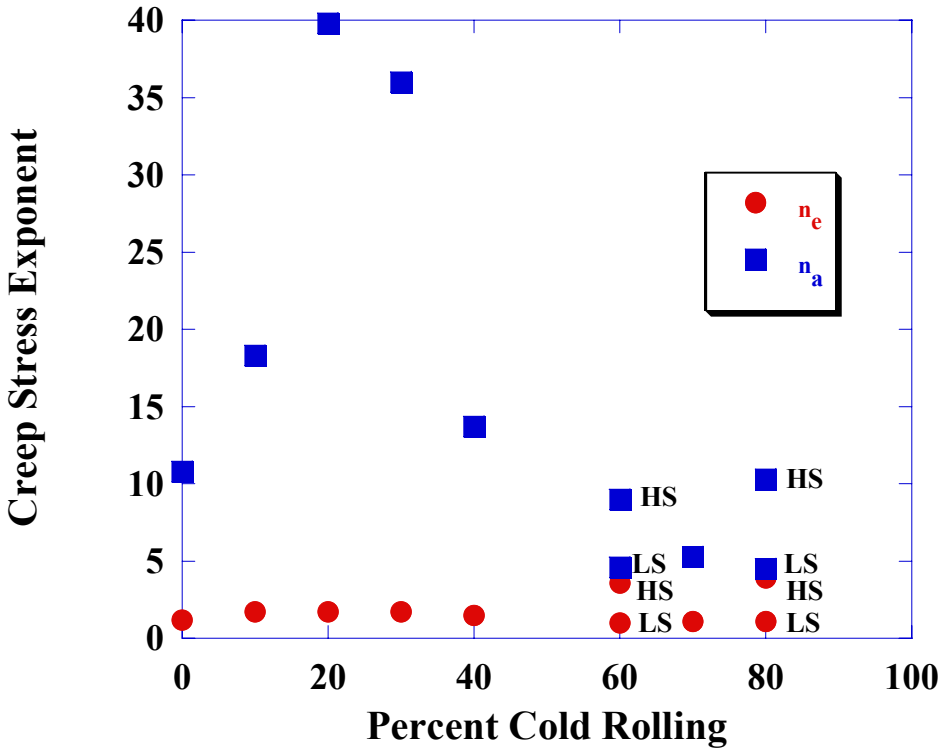

*SPF samples (55-80%CR) are represented in figure at 70%CR. HS represents the high stress creep stress exponent and LS represents the low stress creep stress exponent for cold rolling levels where there are multiple creep stress exponents.

Figure 14. Creep stress exponents for the cold rolled and 954°C annealed then aged IN 718 samples.

2. 1050˚C Annealed Samples

Back stress and n values for all cold rolling levels were determined for the 1050°C annealed then aged samples (Figures 15-18). As shown in Figure 15, the SPF sample exhibited the greatest σ_0 value, 630 MPa, while the 30%CR condition exhibited the lowest σ_0 value, 505 MPa. The backstress values for most samples fell in a narrow band, 550-590 MPa. The samples with the lowest σ_0 values also exhibited the highest strain rates for a given applied stress level (Figure 16). The n_a values ranged from 6 to 32 and the n_e values ranged from 1 to 4 (Figures 16-18).

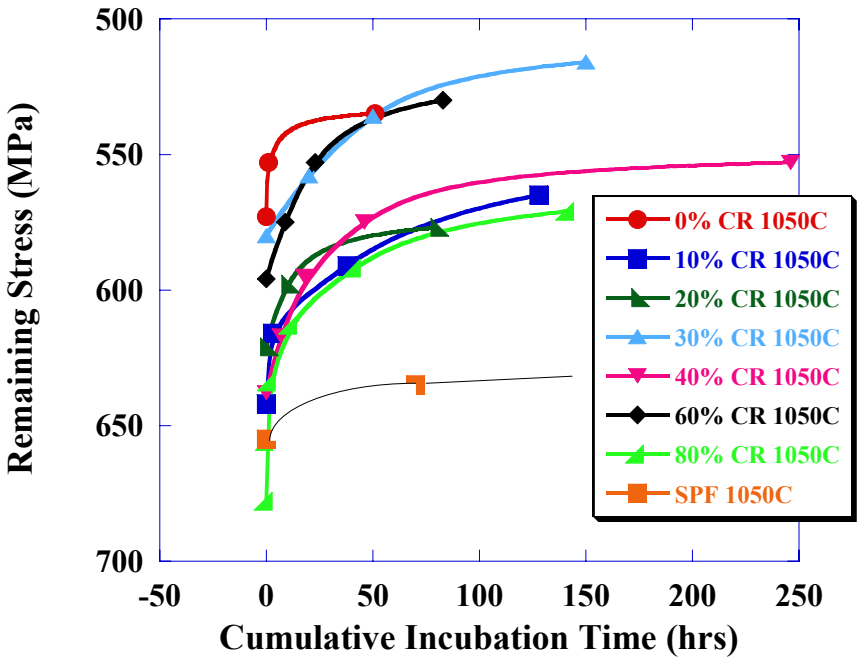

Figure 15. Remaining stress versus cumulative incubation time for the cold rolled and 1050°C annealed then aged IN 718 creep samples.

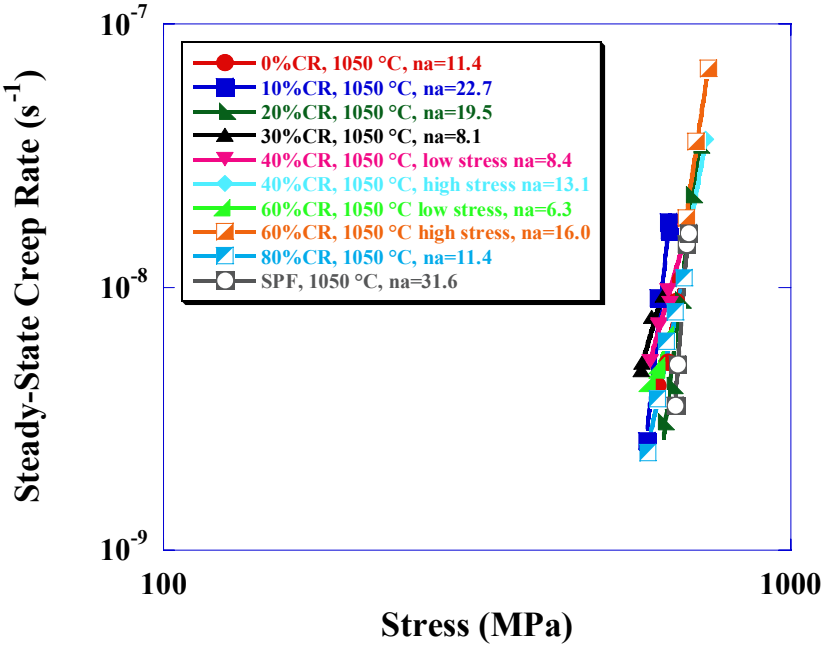

Figure 16. Steady-state creep rate versus applied stress for the cold rolled and 1050°C annealed then aged IN 718 samples.

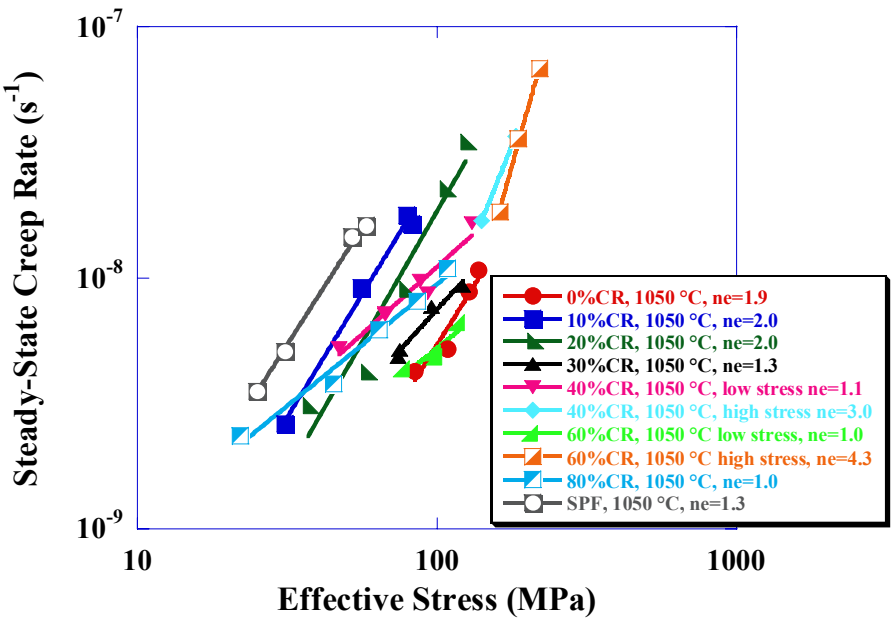

Figure 17. Steady-state creep rate versus effective stress for the cold rolled and 1050°C annealed then aged IN 718 samples.

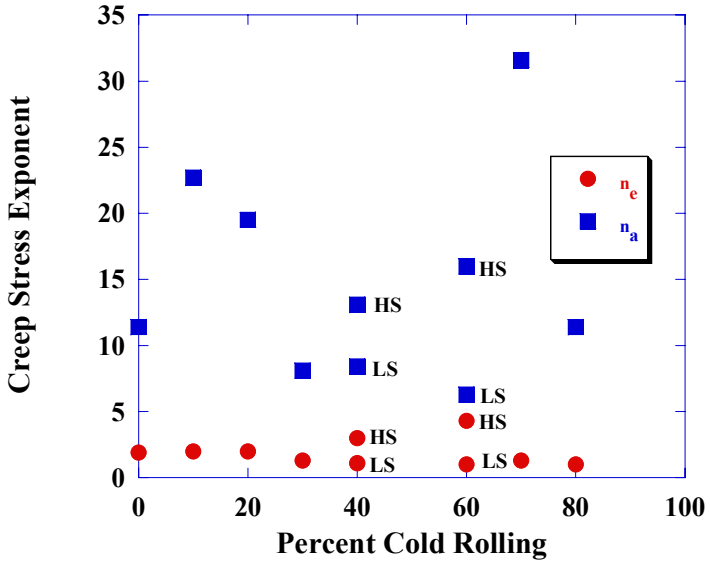

*SPF samples (55-80%CR) are represented in figure at 70%CR. HS represents the high stress creep stress exponent and LS represents the low stress creep stress exponent for cold rolling levels where there are multiple creep stress exponents.

Figure 18. Creep stress exponents for the cold rolled and 1050°C annealed then aged IN 718 samples.

D. Comparisons

The results including a basic discussion have been presented previously. A more detailed discussion including comparisons of the results from the prior sections (i.e. tension, backstress, etc.) will now be presented.

1. Other Work

The strain rates for a given stress level for the 0%CR and 954°C annealed sample agrees well with samples tested under similar conditions by Han and Chatervedi[19, 20] (Figure 19). Figure 19 illustrates the data of this work alongside the results obtained at 625°C and 650°C by Han and Chatervedi[19, 20] which were interpolated to 638°C.

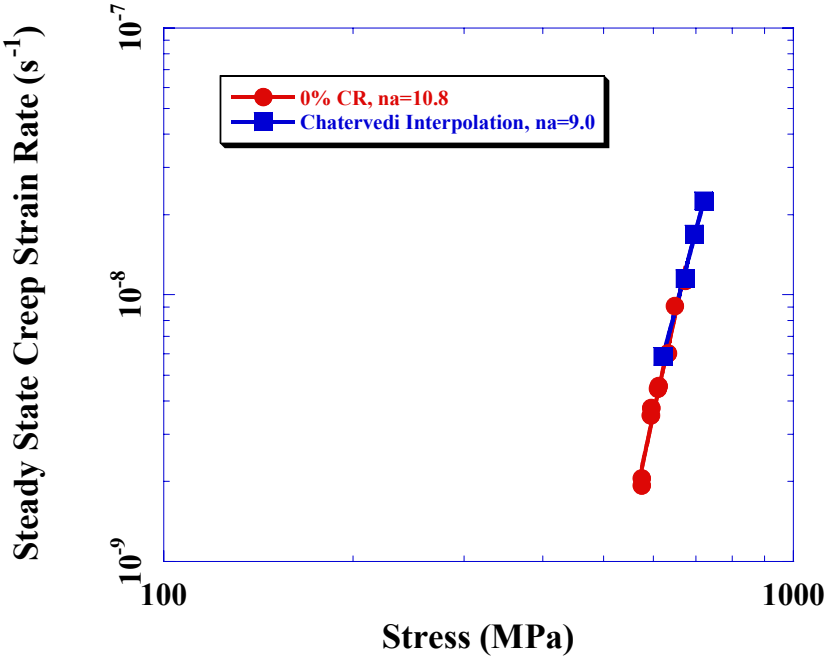

Figure 19. Strain rate comparison between experimental data and the achieved by Han and Chatervedi.[19, 20]

2. Annealing Temperature

The effects of cold rolling on the creep properties of IN 718 for a given annealing temperature were presented previously. A summary of the backstress results as function of cold rolling and annealing temperature is presented in Figure 20. A more detailed discussion of the effect of annealing temperature on a given cold rolling level will follow.

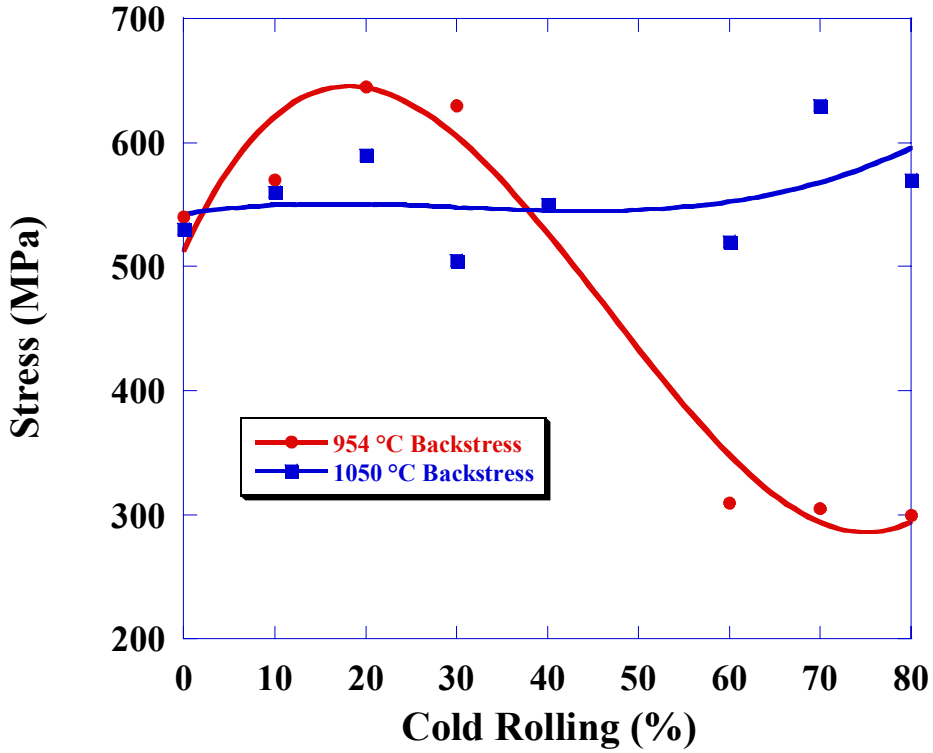

*SPF samples (55-80%CR) are represented in figure at 70%CR.

Figure 20. Backstress as a function of both cold rolling and annealing temperature.

a. High Levels of Cold Rolling

For the 80%CR condition, increasing the annealing temperature from 954°C to 1050°C significantly increased both the backstress and the creep resistance (Figures 21-22). The backstress increased over 90 percent. A similar increase occured for the 60%CR and SPF conditions with an average backstress increase of 88 percent.

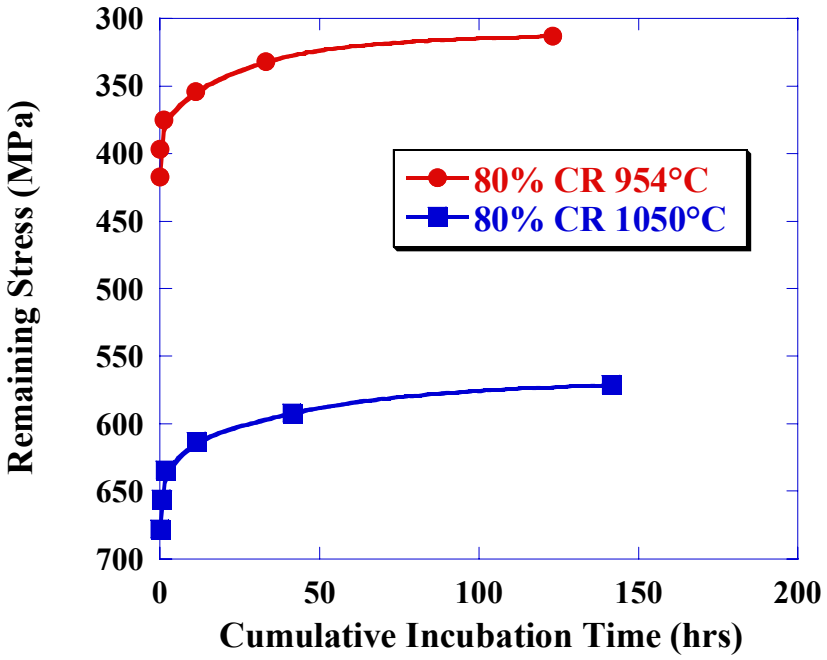

Figure 21. The effect of annealing temperature on the backstress of 80%CR IN 718.

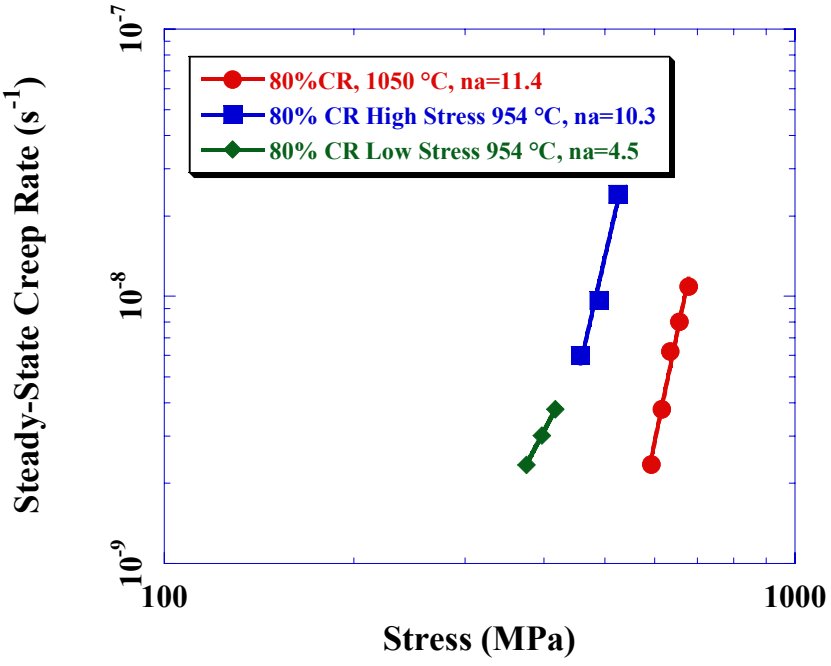

Figure 22. The effect of annealing temperature on the steady-state creep rate of 80%CR IN 718.

b. Low Levels of Cold Rolling

For the 20%CR condition, increasing the annealing temperature from 954°C to 1050°C did not significantly increase the backstress or the creep resistance (Figures 23-24). In fact, the backstress actually decreased approximately 9 percent. The 0-40%CR conditions followed a similar trend and on average actually exhibited a decrease in the backstress of 8 percent.

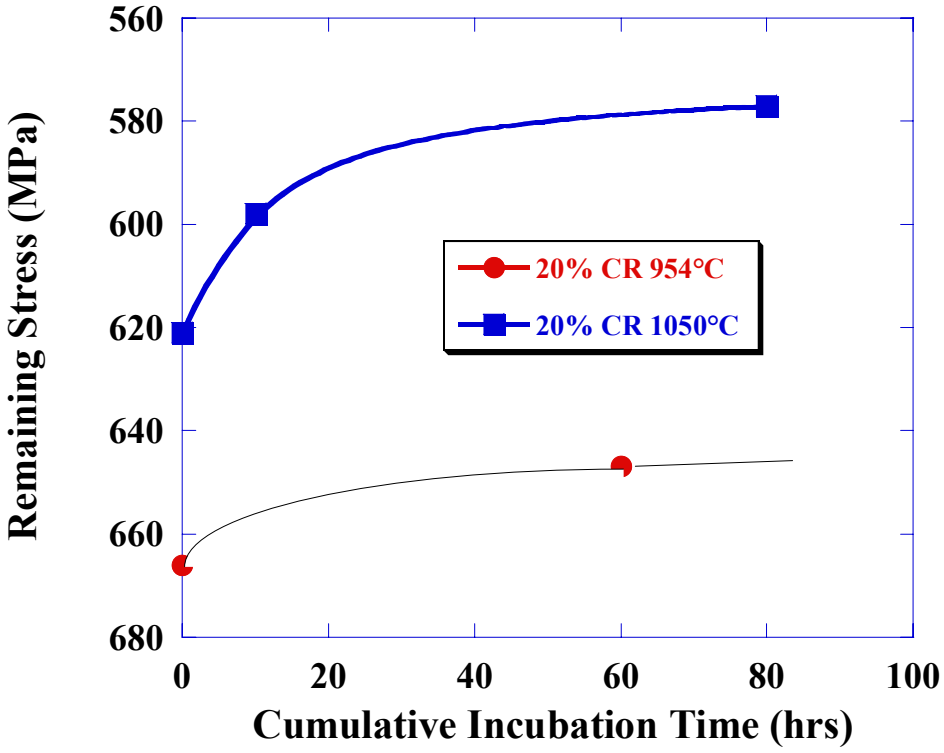

Figure 23. The effect of annealing temperature on the backstress of 20%CR IN 718.

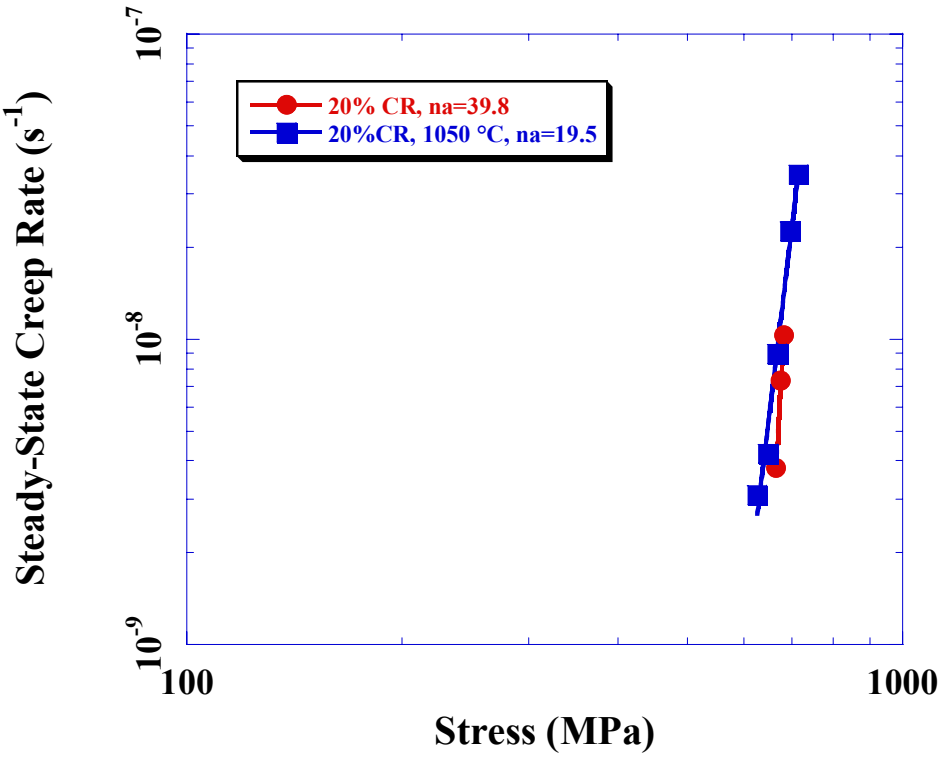

Figure 24. The effect of annealing temperature on the steady-state creep rate of 20%CR IN 718.

3. Transition Stress

As discussed earlier, samples experiencing creep may exhibit a change in mechanism resulting in a change in the stress exponent as the stress level increases. The experimental results (Figure 25) show that n_e was measured to be between one and two for σ_e less than 135 MPa, and n_e was 3.6-3.9 for σ_e greater than 135 MPa. It is important to note that this trend occured independent of annealing temperature and cold rolling deformation.

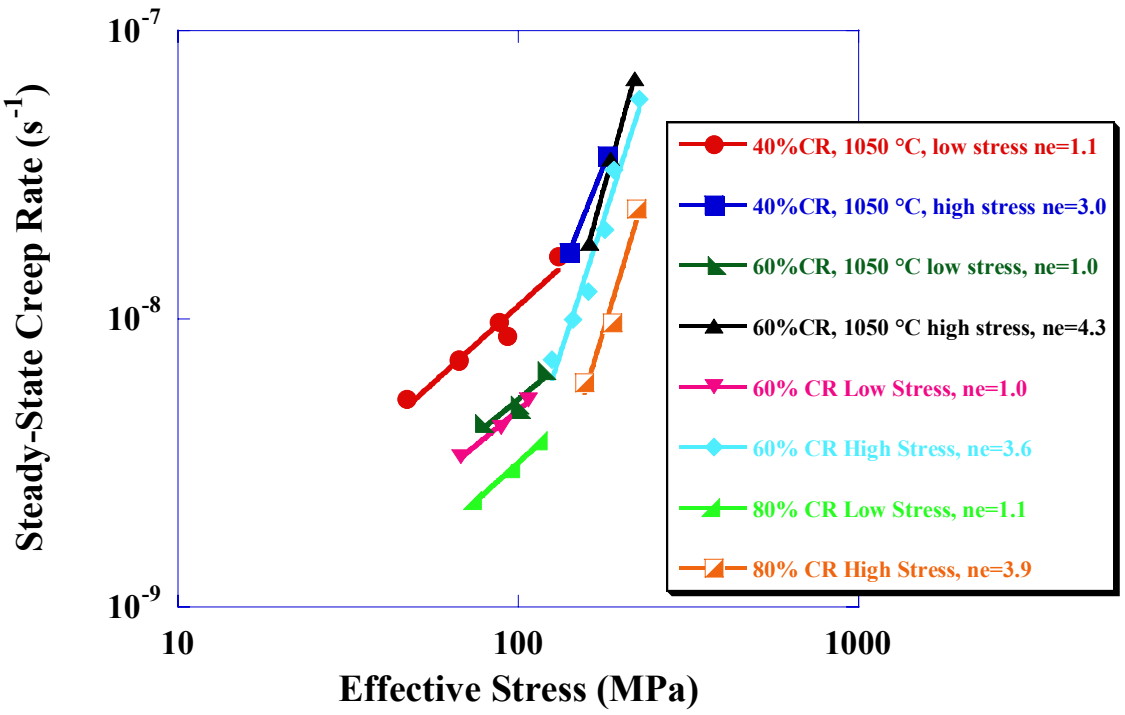

Figure 25. Steady-state creep rate versus effective stress for the cold rolled and annealed then aged IN 718 samples showing a transition region at σ_e = 135 MPa .

This result suggests that the creep mechanism may be dependent on σ_e, and the low-stress regime (σ_e<135 MPa) may be dominated by diffusional creep or grain boundary sliding. Thereby grain size is expected to have played a role in the creep strain rates at σ_e<135 MPa. Electron backscattered diffraction (EBSD) characterization revealed that the fraction of special boundaries decreased with increased cold rolling for the 954°C annealed samples and this may have affected the creep resistance as well.[35]

4. Tensile-Backstress Comparisons

The backstress to tensile strength ratios (σ_o/YS and σ_o/UTS) are presented in Figure 26. The 954°C annealed samples show a small increase in both ratios up to a cold rolling level of 30% followed by a precipitous fall to the higher cold rolling levels (60-80%CR). The 1050°C annealed samples show a small initial decrease in both ratios followed by a slight increase all the way to the 80%CR condition.

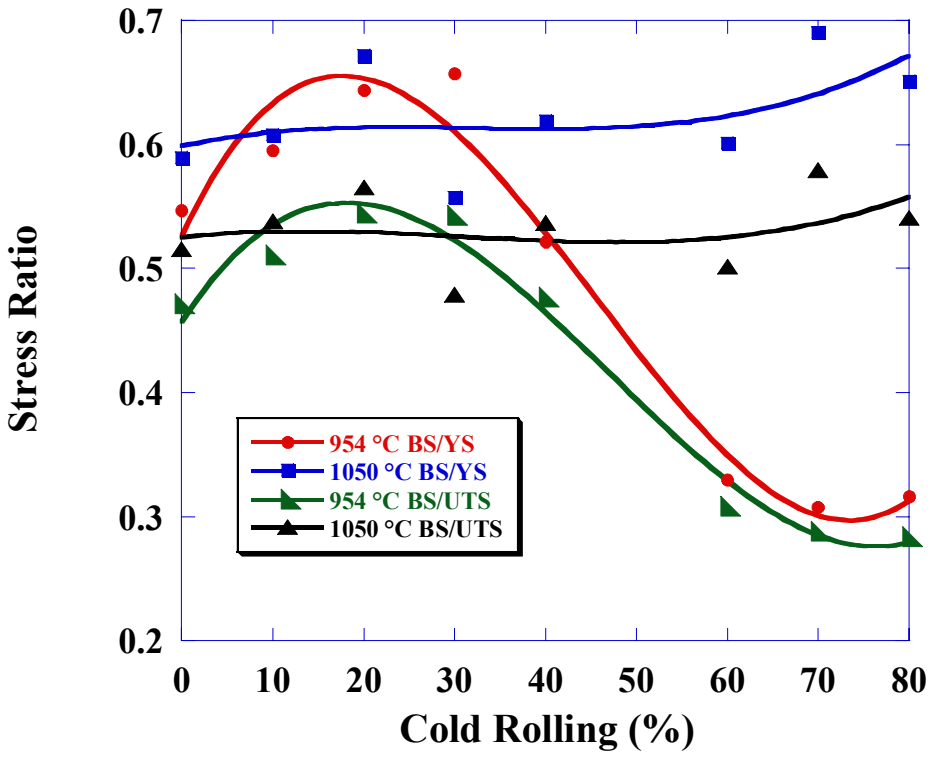

*SPF samples (55-80%CR) are represented in figure at 70%CR.

Figure 26. σ_o/YS and σ_o/UTS as a function of cold rolling for both annealing temperatures.

All samples other than those cold rolled greater than 60%CR and annealed at 954°C exhibited a backstress greater than 50% of the yield stress. This is significant in that yield stress is a typical upper design constraint and these samples will not strain at stress levels below their backstress.

5. Grain Size Comparisons

The trends in YS, UTS, backstress, and grain size with increasing levels of cold rolling for a given annealing temperature are presented in Figures 27 and 28. For the samples annealed at 954°C, the decrease in grain size does not correspond to an increase in YS and UTS. This is opposed to the traditional Hall-Petch relationship. In addition, for samples 20-80%CR, both the grain size and backstress decreased (Note: an increase in ε_{ss} corresponds to a decrease in backstress). This would be expected if grain size were inversely related to ε_{ss} as it should be when diffusional creep is active. For the samples annealed at 1050°C, the grain size did not decrease with increased cold rolling and was

less affected by cold rolling than the samples annealed at 954°C. Thus, it is difficult to speculate on the effect of grain size on the strength and backstress results for the samples annealed at 1050°C.

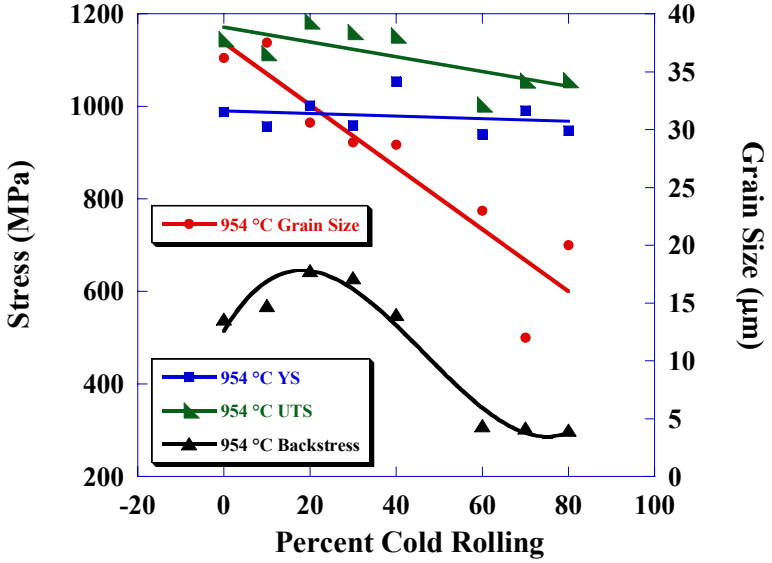

*SPF samples (55-80%CR) are represented in figure at 70%CR.

Figure 27. Trends in YS, UTS, backstress, and grain size with increasing levels of cold rolling for the 954°C annealed then aged IN 718 samples.

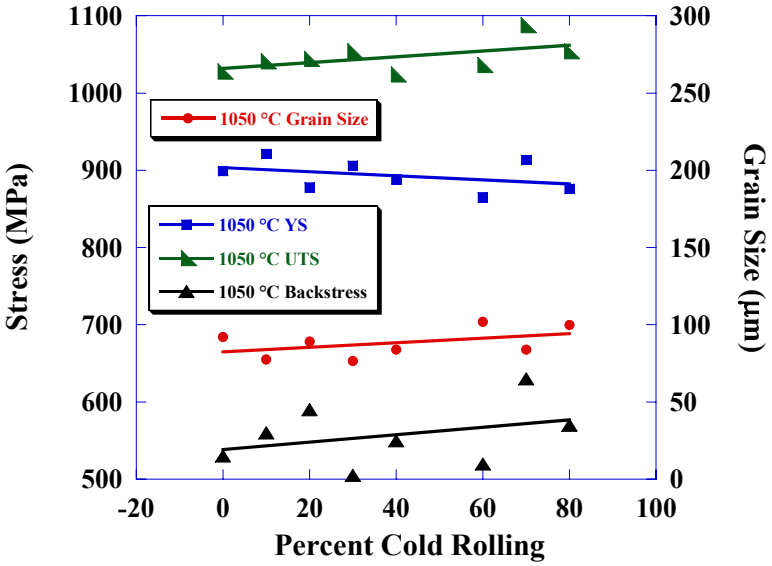

*SPF samples (55-80%CR) are represented in figure at 70%CR.

Figure 28. Trends in YS, UTS, backstress, and grain size with increasing levels of cold rolling for the 1050°C annealed then aged IN 718 samples..

6. Bowing Stress

It has been suggested that the backstress arises from the inability of dislocations to bow between adjacent particles: i.e. that at stresses below the Orwan bowing stress, dislocations will not be able to bow between adjacent particles and positive strain will not occur.[3] For example, according to Evans and Wilshire, $Ni_{20}Cr_2ThO_2$ single crystals will not creep at stresses below its Orwan bowing stress and polycrystalline $Ni_{20}Cr_2ThO_2$ will not creep until its Orwan bowing stress is exceeded locally.[3] These results suggest an effective stress which is equal to the applied stress minus the Orwan bowing stress governs the creep behavior. This is similar to the effective stress presented in Equation 3.

The Orwan bowing stress, τ_{bow}, can be approximated as:[3]

$$\tau_{bow} = Gb/\lambda \qquad (4)$$

where G is the shear modulus, b is the burgers vector, and λ is the mean interparticle spacing. It is important to note that λ varies with particle size, so this is inherently included in this equation.

Using G = 64 Gpa,[1] b = .3 nm,[36] and λ = 44-56 nm (measured from TEM photos shown in Oblack's et. al. Fig. 2),[37] τ_{bow} values range from 340 to 440 MPa. The significantly higher backstress values observed in this study (up to 645 MPa), suggests there must be other defect/dislocation interactions and/or diffusion barriers that contribute to the backstress in addition to the Orwan bowing stress. A very detailed TEM investigation beyond the scope of this thesis would be required to determine the exact cause of this backstress.

IV SUMMARY AND CONCLUSIONS

The purpose of this study was to determine the processing-microstructure-property relationships of IN 718. The following results and conclusions were reached:

- The backstress and creep resistance of IN 718 are strongly dependent on sheet processing.

  954°C Annealed

  - The 20%CR and 30%CR samples exhibited the greatest σ_0 values, 645 and 630 MPa, respectively, while the 60%CR and 80%CR conditions exhibited the lowest σ_0 values, which were less than half those of the highest σ_0 values.
  - The creep resistance after 60-80%CR is significantly worse than conventionally processed and 10%CR, which is expected based on the finer grain size of the heavily CR samples.
  - The samples with the lowest σ_0 values also exhibited the highest strain rates for a given applied stress level.

  1050°C Annealed

  - The SPF sample exhibited the greatest σ_0 value, 630 MPa, while the 0%CR condition exhibited the lowest σ_0 value, 450 MPa.
  - The backstress values for most samples fell in a narrow band, 550-590 MPa.
  - The samples with the lowest σ_0 values also exhibited the highest strain rates for a given applied stress level.
- For most samples, the backstress was over 50% of the yield stress at 650°C and was as high as 66% for the 30% cold rolled, 954°C annealed condition.
- The significantly higher backstress values in relation to the Orwan bowing stress observed in this study suggests there must be other defect/dislocation interactions and/or diffusion barriers that contribute to the backstress in addition to the Orwan bowing stress.

- A transition in the effective stress exponent occurs regardless of annealing temperature at an effective stress of approximately 135 MPa.
- The decrease in backstress with increased cold rolling observed in the samples annealed at 954°C may be as a result of the corresponding decrease in grain size.
- The data suggest that the creep mechanism is dependent on the effective stress. Accounting for the backstress, the σ_{eff} vs ε_{ss} behavior indicated that diffusional creep or grain boundary sliding may be active at lower stresses; n_e values ranged from 1-2 for $0 < \sigma_{eff} < 135$MPa.
- The 20%CR and 30%CR exhibit the best elevated temperature properties in the 954°C annealed condition.
- IN 718SPF exhibits exceptional strength and creep resistance in the 1050°C annealed condition, on par with the 20-30%CR 954°C annealed samples.

V FUTURE WORK

Future work will include:

- Creep experiments at different temperatures to confirm that observed trends occur for other test temperatures.
- Additional TEM examinations to further predict and confirm mechanisms.
- EBSD work to further relate results to grain boundary character distribution.

REFERENCES

1. *Inconel® Alloy 718, Properties Handbook*, 4th ed. INCO Alloys International, Huntington, WV, 1985.

2. E.A. Loria, "The Status and Prospects of Alloy 718," *J. Met.,* **40** [7] 36-41 (1988).

3. R.W. Evans and B. Wilshire, *Creep of Metals and Alloys*. The Institute of Metals, New York, NY, 1985.

4. R.W. Hertzberg, *Deformation and Fracture Mechanics of Engineering Materials*; Ch. 5. John Wiley and Sons, New York, NY, 1996.

5. A.K. Mukherjee, J.E. Bird, and J.E. Dorn, "Experimental Correlations for High Temperature Creep," *Trans. Am. Soc. Met.*, **62** 155-79 (1969).

6. K.R. Williams and B. Wilshire, "On the Stress- and Temperature-Dependence of Creep of Nimonic 80A," *Met. Sci. J.,* **7** [9] 176-9 (1973).

7. J.D. Parker and B. Wilshire, "Effect of a Dispersion of Cobalt Particles on High-Temperature Creep of Copper," *Met. Sci. J.,* **9** [5] 248-52 (1975).

8. P.W. Davies, G. Nelmes, K.R. Williams and B. Wilshire, "Stress-Change Experiments during High-Temperature Creep of Copper, Iron, and Zinc," *Met. Sci. J.,* **7** [5] 87-92 (1973).

9. W.J. Evans and G.F. Harrison, "Development of a Universal Equation for Secondary Creep Rates in Pure Metals and Engineering Alloys," *Met. Sci. J.,* **10** [9] 307-13 (1976).

10. R. Lagneborg and B. Bergman, " Stress/Creep Rate Behaviour of Precipitation-Hardened Alloys," *Met. Sci. J.,* **10** [1] 20-28 (1976).

11. D.D. Sherby and P.M. Burke, " Mechanical Behavior of Crystalline Solids at Elevated Temperature,"*Prog. Mater. Sci.,* **13** 323-90 (1968).

12. J.D. Parker and B. Wilshire, "Friction-Stress Measurements during High-Temperature Creep of Polycrystalline Copper," *Met. Sci.,* **12** [10] 453-8 (1978).

13. R. Lund and W.D. Nix, "High Temperature Creep of Ni-20Cr-2ThO_2 Single Crystals," *Acta Mater.,* **24** [5] 469-81 (1976).

14. C.N. Ahlquist and W.D. Nix, "The Measurement of Internal Stresses during Creep of Al and Al-Mg Alloys," *Acta Metall.,* **19** [4] 373-85 (1971).

15. C.L. Meyers, J.C. Shyne, and O.D. Sherby: *Aust. Inst. Met*., 8 (1963) 171.
As cited in Y. Han and M.C. Chaturvedi, "Steady State Creep Deformation of Superalloy Inconel 718," *Mater. Sci. Eng.,* **89** [5] 25-33 (1987).

16. B.A. Wilcox and A.H. Clauer: *Trans. Metall. Soc. AIME*, 236 (1966) 570.
As cited in Y. Han and M.C. Chaturvedi, "Steady State Creep Deformation of Superalloy Inconel 718," *Mater. Sci. Eng.,* **89** [5] 25-33 (1987).

17. A.H. Clauer and B.A. Wilcox: *Met. Sci. J*., 1 (1967) 86.
As cited in Y. Han and M.C. Chaturvedi, "Steady State Creep Deformation of Superalloy Inconel 718," *Mater. Sci. Eng.,* **89** [5] 25-33 (1987).

18. B.A. Wilcox and A.H. Clauer: *Met. Sci. J*., 3 (1969) 26.
As cited in Y. Han and M.C. Chaturvedi, "Steady State Creep Deformation of Superalloy Inconel 718," *Mater. Sci. Eng.,* **89** [5] 25-33 (1987).

19. Y. Han and M. C. Chaturvedi, "A Study of Back Stress during Creep Deformation of a Superalloy Inconel 718," *Mater. Sci. Eng.,* **85** [1-2] 59-65 (1987).

20. Y. Han and M.C. Chaturvedi, "Steady State Creep Deformation of Superalloy Inconel 718," *Mater. Sci. Eng.,* **89** [5] 25-33 (1987).

21. W. Chen and M. C. Chaturvedi, "The Effect of Grain Boundary Precipitates on the Creep Behavior of Inconel 718," *Mater. Sci. Eng.,* **A183** [1-2] 81-89 (1994).

22. J.C. Gibeling and W.D. Nix, "The Description of Elevated Temperature Deformation in Terms of Threshold Stresses and Back Stresses: A Review," *Mater. Sci. Eng.,* **45** [2] 123-35 (1980).

23. S. Purushothaman and J.K. Tien, "Role of Back Stress in the Creep Behavior of Particle Strengthened Alloys," *Acta Mater.,* **26** [4] 519-28 (1978).

24. J.H. Hausselt and W.D. Nix, "Dislocation Structure of Ni-20Cr-2ThO_2 after High Temperature Deformation," *Acta Mater.,* **25** [6] 595-607 (1977).

25. J.E. Harris, “Inhibition of Diffusion Creep by Precipitates,” *Met. Sci. J.,* **7** [1] 1-6 (1973).

26. B. Burton, " On the Mechanism of the Inhibition of Diffusional Creep by Second Phase Particles," *Mater. Sci. Eng.,* **11** [6] 337-43 (1973).

27. G.S. Ansel and J. Weertman, *Trans. Metall. Soc. AIME*, 215 (1959) 838.
As cited in Y. Han and M.C. Chaturvedi, "Steady State Creep Deformation of Superalloy Inconel 718," *Mater. Sci. Eng.,* **89** [5] 25-33 (1987).

28. M.F. Ashby and H.J. Frost: in A.S. Argon (ed.), Constituitive Equations in Plasticity, Massachusetts Institute of Technology Press, Cambridge, MA, 1975, p.117. As cited in Y. Han and M.C. Chaturvedi, "Steady State Creep Deformation of Superalloy Inconel 718," *Mater. Sci. Eng.,* **89** [5] 25-33 (1987).

29. C. Boehlert, Alfred University, December, 2003, Private Communication.

30. G.D. Smith and D.H. Yates, "Superplastic Forming of Inconel Alloy 718SPF" pp. M207-M218 in Advancements in Synthesis and Processes. Society for the Advancement of Material and Process Engineering, Covina, CA, 1992.

31. G.D. Smith and H.L. Flower, "Superplastic Forming of Inconel Alloy 718SPF" pp. 355-364 in Superalloys 718, 625, 706 and Various Derivatives. The Minerals, Metals and Materials Society, Warrendale, PA, 1994.

32. B.A. Baker, INCO Alloys International Technical Investigation, Report No. BAB1323093, Huntington, WV, September, 1993.

33. Y. Huang and P.L. Blackwell, "Microstructure Development and Superplasticity in Inconel 718 Sheet," *Mater. Sci. Technol.,* **19** [4] 461-6 (2003).

34. J.E. Hilliard, "Estimating Grain Size by the Intercept Method," *Met. Prog.,* **78** [5] 99-100 (1964).

35. S. Civelekoglu, "The Use of Electron Backscatter Diffraction for Understanding the Effect of Cold Rolling and Annealing on the Grain Boundary Character Distribution of Inconel Alloy 718"; M.S. Thesis. Alfred University, Alfred, NY 2003.

36. C. Mercer, A.B.O. Soboyejo, and W.O. Soboyejo, "Micromechanisms of Fatigue Crack Growth in a Forged Inconel 718 Nickel-based Superalloy," *Mater. Sci. Eng.,* **A270** [2] 308-22 (1999).

37. J.M. Oblack, D.F. Paulonis, and D.S. Duvall, "Coherency Strengthening in Ni Base Alloys Hardened by DO_{22} γ" Precipitates," *Met. Trans.,* **5** [1] 143-53 (1974).

APPENDIX

Table V. The 638°C Creep Data of IN 718 Samples Annealed at 954°C

Cold Rolling Deformation,%	σ_a, MPa	σ_o, MPa	$\sigma_o - \sigma_a$, MPa	ε_{ss}	n_e	n_a
0%	574	540	34	2.1E-09	1.2	10.8
	574	540	34	1.9E-09	1.2	10.8
	594	540	54	3.5E-09	1.2	10.8
	595	540	55	3.8E-09	1.2	10.8
	609	540	69	4.4E-09	1.2	10.8
	611	540	71	4.6E-09	1.2	10.8
	632	540	92	6.0E-09	1.2	10.8
	649	540	109	9.1E-09	1.2	10.8
	674	540	134	1.1E-08	1.2	10.8
10%	591	570	21	1.0E-09	1.7	18.3
	596	570	26	1.1E-09	1.7	18.3
	610	570	40	2.8E-09	1.7	18.3
	634	570	64	5.1E-09	1.7	18.3
	666	570	96	1.1E-08	1.7	18.3
	694	570	124	1.9E-08	1.7	18.3
20%	666	645	21	3.8E-09	1.7	39.8
	676	645	31	7.3E-09	1.7	39.8
	683	645	38	1.0E-08	1.7	39.8
30%	648	630	28	1.5E-09	1.7	36.0
	668	630	38	5.6E-09	1.7	36.0
	680	630	50	8.4E-09	1.7	36.0
40%	578	550	28	2.4E-09	1.5	13.7
	593	550	43	2.9E-09	1.5	13.7
	596	550	46	2.8E-09	1.5	13.7
	598	550	48	3.3E-09	1.5	13.7
	610	550	60	4.7E-09	1.5	13.7
	613	550	63	5.2E-09	1.5	13.7
	613	550	63	4.8E-09	1.5	13.7
	627	550	77	6.6E-09	1.5	13.7
60%	378	310	68	3.3E-09	1.0	4.6
	399	310	89	4.2E-09	1.0	4.6
	417	310	107	5.2E-09	1.0	4.6
	436	310	126	7.2E-09	3.6	9.0
	455	310	145	9.9E-09	3.6	9.0
	471	310	161	1.2E-08	3.6	9.0
	490	310	180	2.0E-08	3.6	9.0
	501	310	191	3.3E-08	3.6	9.0
	537	310	227	5.8E-08	3.6	9.0
	564	310	254	7.9E-08	3.6	9.0
	598	310	288	1.2E-07	3.6	9.0
	612	310	302	1.3E-07	3.6	9.0
80%	375	300	75	2.3E-09	1.1	4.5
	397	300	97	3.0E-09	1.1	4.5
	417	300	117	3.8E-09	1.1	4.5
	457	300	157	6.0E-09	3.9	10.3
	489	300	189	9.7E-09	3.9	10.3
	523	300	223	2.4E-08	3.9	10.3
Han and Chatervedi [19,20] Interpolation to 638°C	620	524	96	5.9E-09	1.9	9.0
	673	524	149	1.2E-08	1.9	9.0
	696	524	172	1.7E-08	1.9	9.0
	720	524	196	2.3E-08	1.9	9.0
IN 718SPF	334	305	29	2.1E-09	1.1	5.3
	374	305	69	3.3E-09	1.1	5.3
	405	305	100	6.0E-09	1.1	5.3

Table VI. The 638°C Creep Data of IN 718 Samples Annealed at 1050°C

Cold Rolling Deformation,%	σ_a, MPa	σ_o, MPa	$\sigma_o - \sigma_a$, MPa	ε_{ss}	n_a	n_e
0% 1050°C	614	530	84	4.2E-09	11.4	1.9
	638	530	108	5.2E-09	11.4	1.9
	658	530	128	8.8E-09	11.4	1.9
	668	530	138	1.1E-08	11.4	1.9
10% 1050°C	591	560	31	2.6E-09	22.7	2.0
	616	560	56	9.1E-09	22.7	2.0
	639	560	79	1.8E-08	22.7	2.0
	642	560	82	1.6E-08	22.7	2.0
20% 1050°C	627	590	37	3.1E-09	19.5	2.0
	648	590	58	4.2E-09	19.5	2.0
	668	590	78	9.0E-09	19.5	2.0
	696	590	106	2.3E-08	19.5	2.0
	715	590	125	3.5E-08	19.5	2.0
30% 1050°C	579	505	74	4.8E-09	8.1	1.3
	580	505	75	5.2E-09	8.1	1.3
	601	505	96	7.7E-09	8.1	1.3
	627	505	122	9.3E-09	8.1	1.3
40% 1050°C	597	550	47	5.2E-09	8.4	1.1
	617	550	67	7.2E-09	8.4	1.1
	617	550	67	7.1E-09	8.4	1.1
	638	550	88	9.7E-09	8.4	1.1
	643	550	93	8.7E-09	8.4	1.1
	681	550	131	1.6E-08	8.4	1.1
	691	550	141	1.7E-08	13.1	3.0
	733	550	183	3.7E-08	13.1	3.0
60% 1050°C	598	520	78	4.3E-09	6.3	1.0
	619	520	99	5.0E-09	6.3	1.0
	620	520	100	4.8E-09	6.3	1.0
	639	520	119	6.6E-09	6.3	1.0
	682	520	162	1.8E-08	16.0	4.3
	707	520	187	3.6E-08	16.0	4.3
	740	520	220	6.8E-08	16.0	4.3
80% 1050°C	592	570	22	2.35E-09	11.4	1.0
	615	570	45	3.78E-09	11.4	1.0
	634	570	64	6.22E-09	11.4	1.0
	656	570	86	8.05E-09	11.4	1.0
	678	570	108	1.09E-08	11.4	1.0
SPF 1050°C	655	630	25	3.5E-09	31.6	1.3
	661	630	31	5.1E-09	31.6	1.3
	682	630	52	1.5E-08	31.6	1.3
	688	630	58	1.6E-08	31.6	1.3

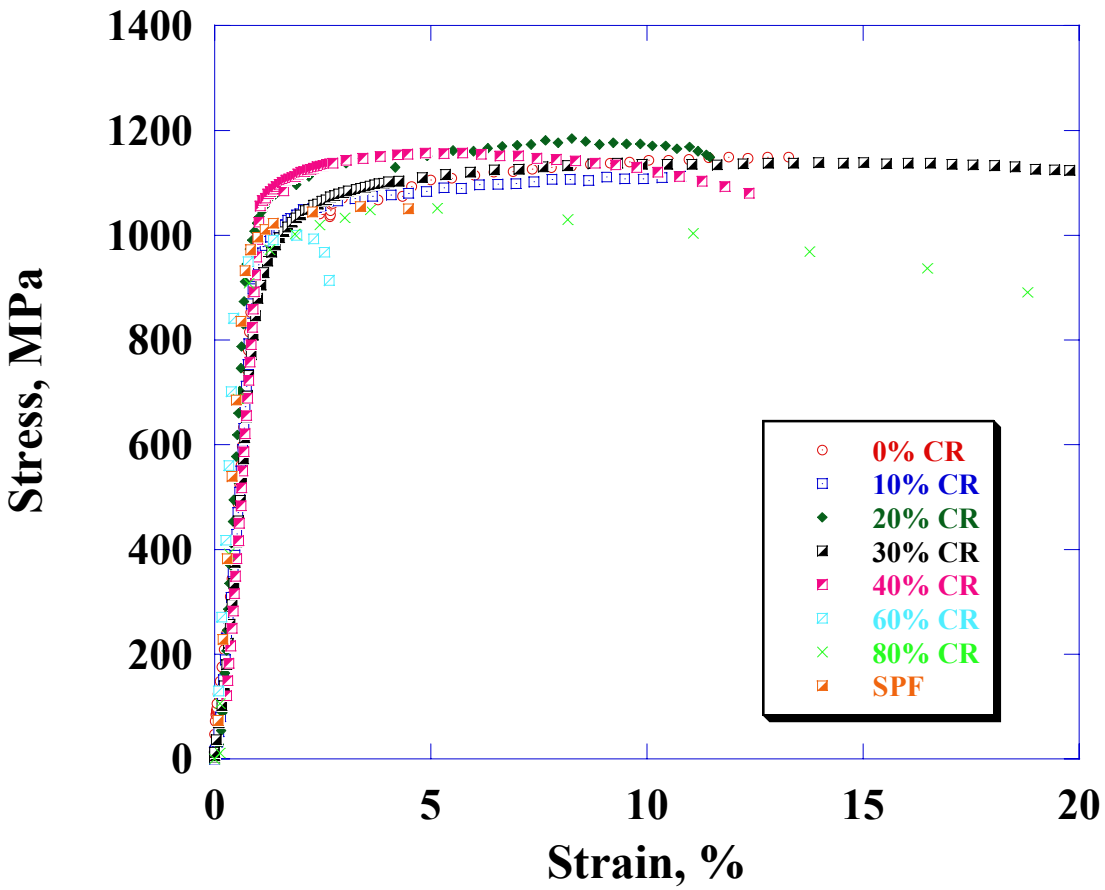

Figure 29. Stress vs strain plot for tensile tests of samples annealed at 954°C.

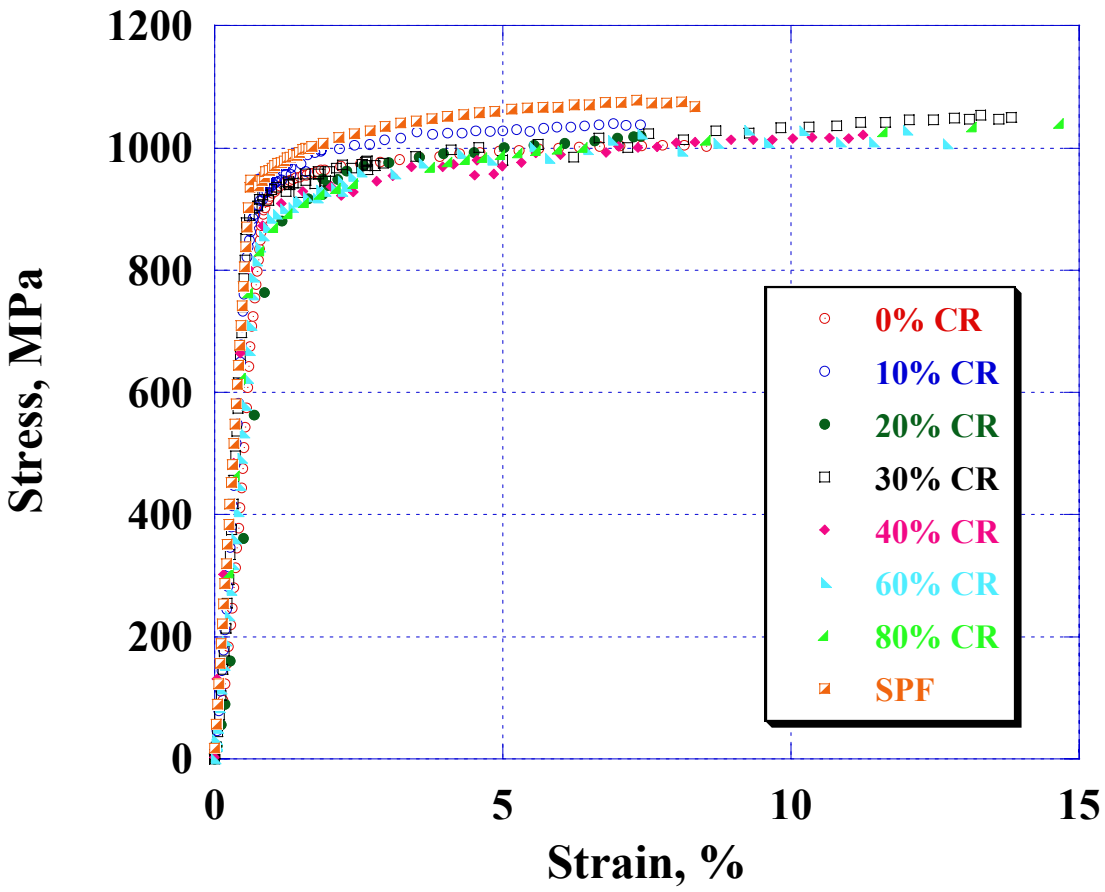

Figure 30. Stress vs strain plot for tensile tests of samples annealed at 1050°C.